Multiscale Cosmic-Ray Transport and Non-linear Feedback

Benedikt Schroer

Supervisor: Pasquale Blasi

Co-Supervisor: Carmelo Evoli

December 15, 2022

Content

1. Introduction
2. Phenomenological Approach to CR transport in the Galaxy
3. Non-linear theory of CRs escaping a SNR
4. TeV Halos
5. Conclusions and Outlook

Introduction

Observations

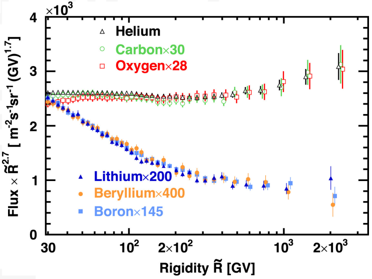

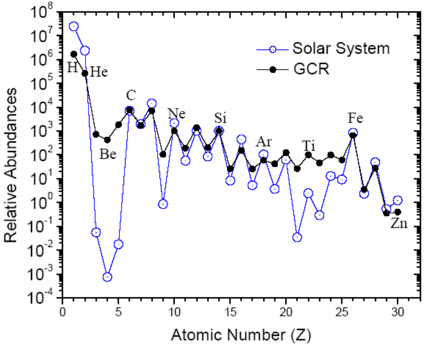

- The overabundant elements show steeper spectra than the other nuclei
- Interpretation of these observations: The secondary CRs are produced via spallation of primaries

[AMS Collaboration 2021; http://www.srl.caltech.edu]

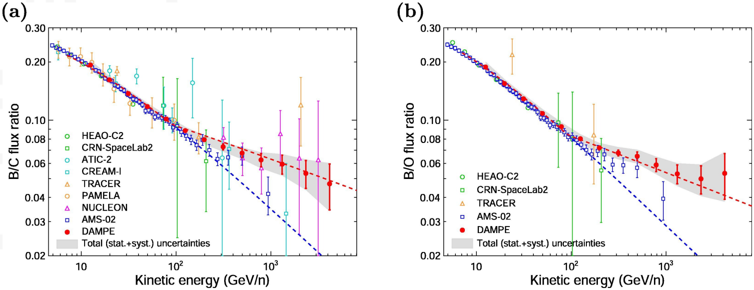

- Secondary over primary ratios let you infer a grammage = traversed column density of CRs on their way to Earth
- energy dependent quantity

[DAMPE Collaboration 2022]

Residence Time

- Presence of radioactive nuclei can give hints about residence time of CRs in the Galaxy
- Production cross sections of Be isotopes are comparable, but ^{10}Be has a half time of $\tau_d \sim 2\,$Myrs
- $\Rightarrow$ ^{10}Be/^{9}Be ratio depends on confinement time of CRs in the Galaxy

Residence Time

- Presence of radioactive nuclei can give hints about residence time of CRs in the Galaxy
- Production cross sections of Be isotopes are comparable, but ^{10}Be has a half time of $\tau_d \sim 2\,$Myrs
- $\Rightarrow$ ^{10}Be/^{9}Be ratio depends on confinement time of CRs in the Galaxy
- Measurements show this ratio to be roughly ~ 0.1 at 100 MeV/n, suggesting a residence time much larger than τ_d [Connell 1998]
- On the other hand, CRs would accumulate the inferred grammage in the disc after $\sim X/(nmc) \approx 2\,$Myrs$\sim \tau_D$
  $\Rightarrow$ CRs spend at least part of their life in low density environments

Standard Picture of CR Transport

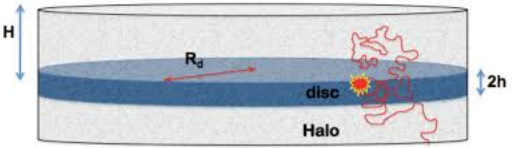

Standard Picture of CR Transport

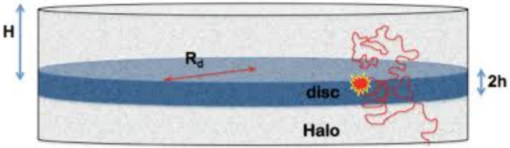

$$\underbrace{-\frac{\partial}{\partial z}\left[D_a \frac{\partial f_a}{\partial z}\right]}_{\text{Diffusion}} + \underbrace{\frac{\mu v(p)\sigma_a}{m}\delta(z) f_a}_{\text{Spallation losses}} = \underbrace{2h_d q_{0,a}(p)\delta(z)}_{\text{Injection at the sources}} + \underbrace{\sum_{a'>a} \frac{\mu\, v(p)\sigma_{a'\to a}}{m}\delta(z) f_{a'}}_{\text{Production via Spallation}}$$

- What causes diffusion of charged particles?

GSSI

Standard Picture of CR Transport

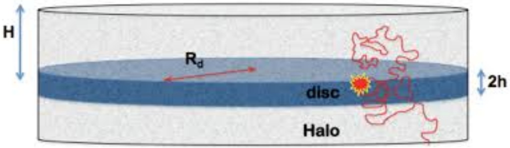

$$\underbrace{-\frac{\partial}{\partial z}\left[D_a \frac{\partial f_a}{\partial z}\right]}_{\text{Diffusion}} + \underbrace{\frac{\mu v(p)\sigma_a}{m}\delta(z) f_a}_{\text{Spallation losses}} = \underbrace{2h_d q_{0,a}(p)\delta(z)}_{\text{Injection at the sources}} + \underbrace{\sum_{a'>a} \frac{\mu\, v(p)\sigma_{a'\to a}}{m}\delta(z) f_{a'}}_{\text{Production via Spallation}}$$

- What causes diffusion of charged particles? $\rightarrow$ resonant scattering off magnetic perturbations
- Resonance condition: $k_{\text{res}} = 1/r_L$
- Diffusion coefficient

$$D = \frac{1}{3}\frac{v r_L}{P(k_{\text{res}})} \propto \frac{1}{\delta B^2}$$

Magnetic Turbulence

- Different types of turbulence, e.g., extrinsic turbulence from, e.g., SNR
- Self-generated turbulence: Particles moving in a background plasma can excite electromagnetic waves, that grow exponentially $\rightarrow$ magnetic instabilities
- Instabilities are fundamental for CR physics, for the purpose of this talk we can divide the self-generated turbulence into two types:
  - **Resonant streaming instability** [Kulsrud & Pearce 1969]
  - Grows on resonant scales $k \sim r_L^{-1}$
  - Immediate impact on particle transport
  - **Non-resonant streaming instability** [Bell 2004]
  - Grows on scales much smaller than r_L
  - Impacts transport after saturation and cascading to larger scales

Success of the Standard Model of Transport

- The biggest success of this transport model is how it combines many different observables into one coherent picture
- Secondary and primary nuclei fluxes, as well as fluxes of unstable nuclei are well reproduced
- Connects the inferred presence of turbulent magnetic fields [Rand & Kulkarni 1989] with diffusive behavior of the particles
- Radio emission from high Galactic latitudes can be interpreted as synchrotron emission of diffusing electrons [Orlando & Strong 2013]

Success of the Standard Model of Transport

- The biggest success of this transport model is how it combines many different observables into one coherent picture
- Secondary and primary nuclei fluxes, as well as fluxes of unstable nuclei are well reproduced
- Connects the inferred presence of turbulent magnetic fields [Rand & Kulkarni 1989] with diffusive behavior of the particles
- Radio emission from high Galactic latitudes can be interpreted as synchrotron emission of diffusing electrons [Orlando & Strong 2013]
- New findings can uncover additional effects leading to a more complete picture of transport

Possible Caveat

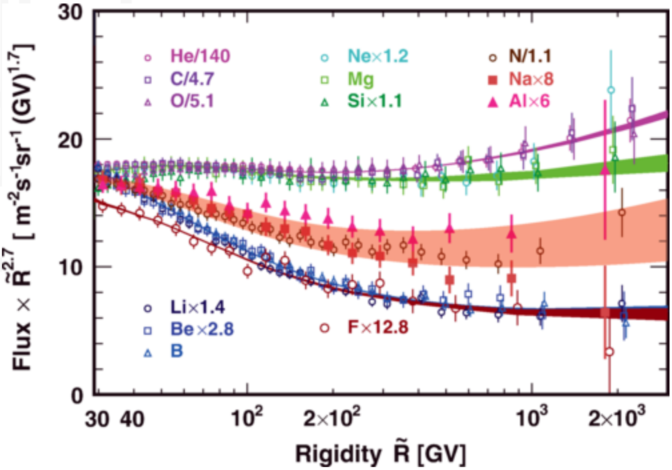

[AMS Collaboration 2021]

Other Possible Caveats

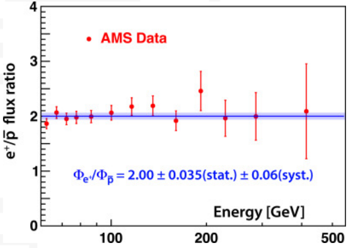

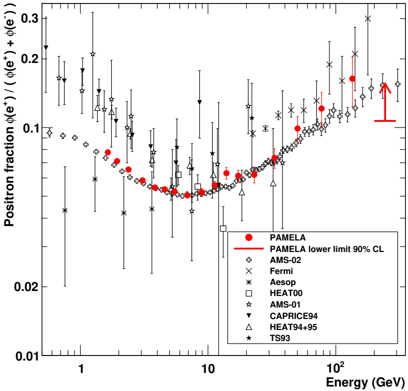

[AMS Collaboration 2021; Pamela Collaboration 2013]

Addressing the Caveats

- It is "natural" to extend the standard model in order to keep the existing agreement with available data

Addressing the Caveats

- It is "natural" to extend the standard model in order to keep the existing agreement with available data
- The slope of antiprotons and positrons motivated speculations about abandoning some of the underlying principles of the standard approach [Cowsik & Burch 2010; Lipari 2017]
- Idea: CRs accumulate most of their grammage close to the sources and an energy-independent grammage during transport
- However, these models need to be tested against all other observations that support the standard model

Phenomenological Approach to CR transport in the Galaxy

CRAMS Model

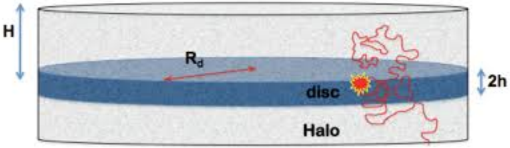

CRAMS Model

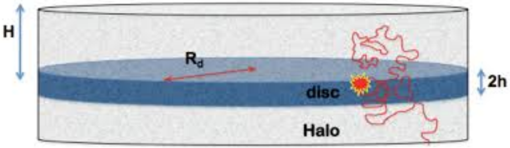

$$-\frac{\partial}{\partial z}\left[D_a\frac{\partial f_a}{\partial z}\right]+v_A\frac{\partial f_a}{\partial z}\quad-\frac{dv_A}{dz}\frac{p}{3}\frac{\partial f_a}{\partial p}$$

$$+\frac{1}{p^2}\frac{\partial}{\partial p}\left[p^2\left(\frac{dp}{dt}\right)_{a,\mathrm{ion}}f_a\right]+\frac{\mu v(p)\sigma_a}{m}\delta(z)f_a\qquad+\frac{f_a}{\hat{\tau}_{d,a}}$$

$$=\quad 2h_d q_{0,a}(p)\delta(z)\quad+\sum_{a'>a}\frac{\mu\, v(p)\sigma_{a'\to a}}{m}\delta(z)f_{a'}\qquad+\sum_{a'>a}\frac{f_{a'}}{\hat{\tau}_{d,a'}}$$

CRAMS Model

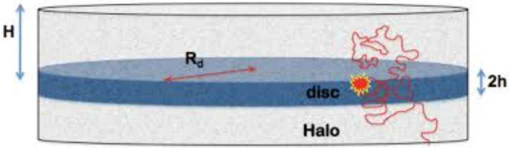

$$
\underbrace{-\frac{\partial}{\partial z}\left[D_a \frac{\partial f_a}{\partial z}\right]}_{\text{Diffusion}} + v_A \frac{\partial f_a}{\partial z} - \frac{dv_A}{dz}\frac{p}{3}\frac{\partial f_a}{\partial p}
$$

$$
+\frac{1}{p^2}\frac{\partial}{\partial p}\left[p^2 \left(\frac{dp}{dt}\right)_{a,\mathrm{ion}} f_a\right] + \frac{\mu v(p)\sigma_a}{m}\delta(z) f_a + \frac{f_a}{\hat{\tau}_{d,a}}
$$

$$
= 2h_d q_{0,a}(p)\delta(z) + \sum_{a'>a} \frac{\mu\, v(p)\sigma_{a'\to a}}{m}\delta(z) f_{a'} + \sum_{a'>a}\frac{f_{a'}}{\hat{\tau}_{d,a'}}
$$

CRAMS Model

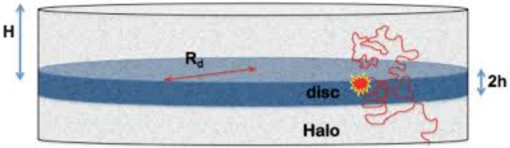

$$
\underbrace{-\frac{\partial}{\partial z}\left[D_a \frac{\partial f_a}{\partial z}\right]}_{\text{Diffusion}} \underbrace{+ v_A \frac{\partial f_a}{\partial z}}_{\text{Advection}} - \frac{dv_A}{dz}\frac{p}{3}\frac{\partial f_a}{\partial p}
$$

$$
+ \frac{1}{p^2}\frac{\partial}{\partial p}\left[p^2 \left(\frac{dp}{dt}\right)_{a,\mathrm{ion}} f_a\right] + \frac{\mu v(p)\sigma_a}{m}\delta(z) f_a + \frac{f_a}{\hat{\tau}_{d,a}}
$$

$$
= 2h_d q_{0,a}(p)\delta(z) + \sum_{a'>a} \frac{\mu\, v(p)\sigma_{a'\to a}}{m}\delta(z) f_{a'} + \sum_{a'>a}\frac{f_{a'}}{\hat{\tau}_{d,a'}}
$$

CRAMS Model

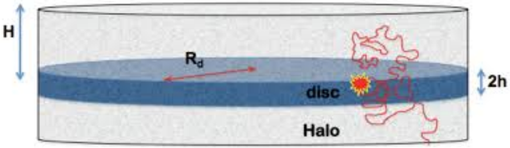

$$\underbrace{-\frac{\partial}{\partial z}\left[D_a \frac{\partial f_a}{\partial z}\right]}_{\text{Diffusion}} \underbrace{+v_A \frac{\partial f_a}{\partial z}}_{\text{Advection}} \underbrace{-\frac{dv_A}{dz}\frac{p}{3}\frac{\partial f_a}{\partial p}}_{\text{Adiabatic E-losses}}$$

$$+\frac{1}{p^2}\frac{\partial}{\partial p}\left[p^2\left(\frac{dp}{dt}\right)_{a,\mathrm{ion}} f_a\right] + \frac{\mu v(p)\sigma_a}{m}\delta(z) f_a \qquad + \frac{f_a}{\hat{\tau}_{d,a}}$$

$$= \quad 2h_d q_{0,a}(p)\delta(z) \quad + \sum_{a'>a} \frac{\mu\, v(p)\sigma_{a'\to a}}{m}\delta(z) f_{a'} \qquad + \sum_{a'>a} \frac{f_{a'}}{\hat{\tau}_{d,a'}}$$

CRAMS Model

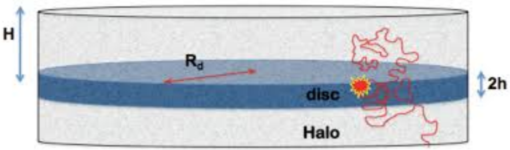

$$
-\underbrace{\frac{\partial}{\partial z}\left[D_a \frac{\partial f_a}{\partial z}\right]}_{\text{Diffusion}} + \underbrace{v_A \frac{\partial f_a}{\partial z}}_{\text{Advection}} - \underbrace{\frac{dv_A}{dz}\frac{p}{3}\frac{\partial f_a}{\partial p}}_{\text{Adiabatic E-losses}}
$$

$$
+ \underbrace{\frac{1}{p^2}\frac{\partial}{\partial p}\left[p^2\left(\frac{dp}{dt}\right)_{a,\mathrm{ion}} f_a\right]}_{\text{Ionization losses}} + \frac{\mu v(p)\sigma_a}{m}\delta(z) f_a + \frac{f_a}{\hat{\tau}_{d,a}}
$$

$$
= 2h_d q_{0,a}(p)\delta(z) + \sum_{a'>a} \frac{\mu\, v(p)\sigma_{a'\to a}}{m}\delta(z) f_{a'} + \sum_{a'>a}\frac{f_{a'}}{\hat{\tau}_{d,a'}}
$$

CRAMS Model

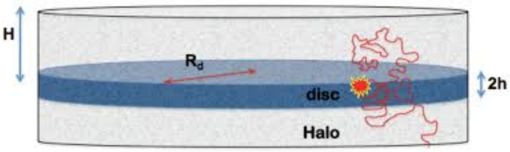

$$\underbrace{-\frac{\partial}{\partial z}\left[D_a\frac{\partial f_a}{\partial z}\right]}_{\text{Diffusion}}\underbrace{+v_A\frac{\partial f_a}{\partial z}}_{\text{Advection}}\underbrace{-\frac{dv_A}{dz}\frac{p}{3}\frac{\partial f_a}{\partial p}}_{\text{Adiabatic E-losses}}$$

$$\underbrace{+\frac{1}{p^2}\frac{\partial}{\partial p}\left[p^2\left(\frac{dp}{dt}\right)_{a,\mathrm{ion}}f_a\right]}_{\text{Ionization losses}}\underbrace{+\frac{\mu v(p)\sigma_a}{m}\delta(z)f_a}_{\text{Spallation losses}}+\frac{f_a}{\hat{\tau}_{d,a}}$$

$$=2h_d q_{0,a}(p)\delta(z)+\sum_{a'>a}\frac{\mu\, v(p)\sigma_{a'\to a}}{m}\delta(z)f_{a'}+\sum_{a'>a}\frac{f_{a'}}{\hat{\tau}_{d,a'}}$$

CRAMS Model

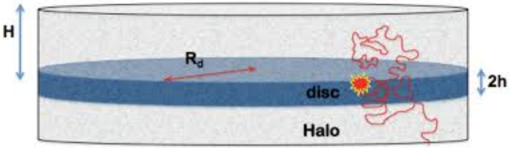

$$\underbrace{-\frac{\partial}{\partial z}\left[D_a\frac{\partial f_a}{\partial z}\right]}_{\text{Diffusion}}\underbrace{+v_A\frac{\partial f_a}{\partial z}}_{\text{Advection}}\underbrace{-\frac{dv_A}{dz}\frac{p}{3}\frac{\partial f_a}{\partial p}}_{\text{Adiabatic E-losses}}$$

$$\underbrace{+\frac{1}{p^2}\frac{\partial}{\partial p}\left[p^2\left(\frac{dp}{dt}\right)_{a,\mathrm{ion}}f_a\right]}_{\text{Ionization losses}}\underbrace{+\frac{\mu v(p)\sigma_a}{m}\delta(z)f_a}_{\text{Spallation losses}}\underbrace{+\frac{f_a}{\hat{\tau}_{d,a}}}_{\text{Radioactive decay}}$$

$$= 2h_d q_{0,a}(p)\delta(z) + \sum_{a'>a}\frac{\mu\, v(p)\sigma_{a'\to a}}{m}\delta(z)f_{a'} + \sum_{a'>a}\frac{f_{a'}}{\hat{\tau}_{d,a'}}$$

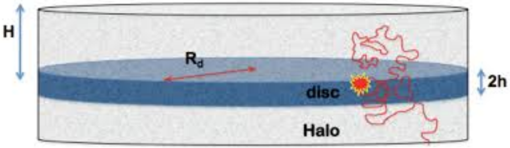

$$
\underbrace{-\frac{\partial}{\partial z}\left[D_a \frac{\partial f_a}{\partial z}\right]}_{\text{Diffusion}} \underbrace{+ v_A \frac{\partial f_a}{\partial z}}_{\text{Advection}} \underbrace{- \frac{dv_A}{dz}\frac{p}{3}\frac{\partial f_a}{\partial p}}_{\text{Adiabatic E-losses}}
$$

$$
\underbrace{+\frac{1}{p^2}\frac{\partial}{\partial p}\left[p^2 \left(\frac{dp}{dt}\right)_{a,\mathrm{ion}} f_a\right]}_{\text{Ionization losses}} \underbrace{+\frac{\mu v(p)\sigma_a}{m}\delta(z) f_a}_{\text{Spallation losses}} \underbrace{+\frac{f_a}{\hat{\tau}_{d,a}}}_{\text{Radioactive decay}}
$$

$$
= \underbrace{2h_d q_{0,a}(p)\delta(z)}_{\text{Injection at the sources}} + \sum_{a'>a} \frac{\mu\, v(p)\sigma_{a'\to a}}{m}\delta(z) f_{a'} + \sum_{a'>a} \frac{f_{a'}}{\hat{\tau}_{d,a'}}
$$

CRAMS Model

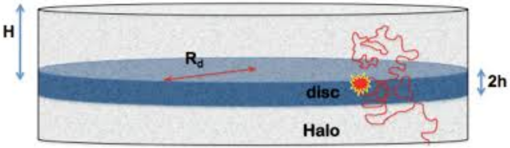

$$
\underbrace{-\frac{\partial}{\partial z}\left[D_a\frac{\partial f_a}{\partial z}\right]}_{\text{Diffusion}}\underbrace{+v_A\frac{\partial f_a}{\partial z}}_{\text{Advection}}\underbrace{-\frac{dv_A}{dz}\frac{p}{3}\frac{\partial f_a}{\partial p}}_{\text{Adiabatic E-losses}}
$$

$$
\underbrace{+\frac{1}{p^2}\frac{\partial}{\partial p}\left[p^2\left(\frac{dp}{dt}\right)_{a,\mathrm{ion}}f_a\right]}_{\text{Ionization losses}}\underbrace{+\frac{\mu v(p)\sigma_a}{m}\delta(z)f_a}_{\text{Spallation losses}}\underbrace{+\frac{f_a}{\hat{\tau}_{d,a}}}_{\text{Radioactive decay}}
$$

$$
=\underbrace{2h_d q_{0,a}(p)\delta(z)}_{\text{Injection at the sources}}\underbrace{+\sum_{a'>a}\frac{\mu\, v(p)\sigma_{a'\to a}}{m}\delta(z)f_{a'}}_{\text{Production via Spallation}}+\sum_{a'>a}\frac{f_{a'}}{\hat{\tau}_{d,a'}}
$$

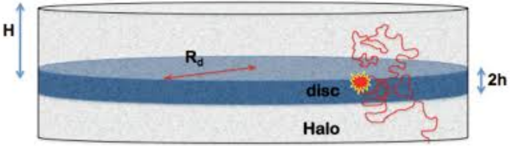

$$\underbrace{-\frac{\partial}{\partial z}\left[D_a \frac{\partial f_a}{\partial z}\right]}_{\text{Diffusion}} \underbrace{+v_A \frac{\partial f_a}{\partial z}}_{\text{Advection}} \underbrace{-\frac{dv_A}{dz}\frac{p}{3}\frac{\partial f_a}{\partial p}}_{\text{Adiabatic E-losses}}$$

$$\underbrace{+\frac{1}{p^2}\frac{\partial}{\partial p}\left[p^2\left(\frac{dp}{dt}\right)_{a,\mathrm{ion}} f_a\right]}_{\text{Ionization losses}} \underbrace{+\frac{\mu v(p)\sigma_a}{m}\delta(z) f_a}_{\text{Spallation losses}} \underbrace{+\frac{f_a}{\hat{\tau}_{d,a}}}_{\text{Radioactive decay}}$$

$$= \underbrace{2h_d q_{0,a}(p)\delta(z)}_{\text{Injection at the sources}} \underbrace{+\sum_{a'>a}\frac{\mu\, v(p)\sigma_{a'\to a}}{m}\delta(z) f_{a'}}_{\text{Production via Spallation}} \underbrace{+\sum_{a'>a}\frac{f_{a'}}{\hat{\tau}_{d,a'}}}_{\text{Production due to decay}}$$

Overview

- Same equation used by different groups with two different approaches: solving the equation numerically [Korsmeier & Cuoco 2021; Boschini et al. 2021; De La Torre Luque et al. 2022] or semianalytically [Evoli et al. 2019; Weinrich et al. 2020; Schroer et al. 2021, PRD]
- Big differences can arise from different cross-section models used
- Uncertainties in production cross sections of $\sim 20 - 30\,\%$ are often limiting factor to reach conclusions
- Focus has been on elements lighter than O but since the release of AMS-02 data of heavier nuclei, the whole nucleus chain was incorporated into the models [Boschini et al. 2021; Schroer et al. 2021, PRD; De La Torre Luque et al. 2022]
- Main difference in our analysis: All primaries are injected with the same slope γ, expected from zeroth order diffuse shock acceleration

Fit to light Ratios

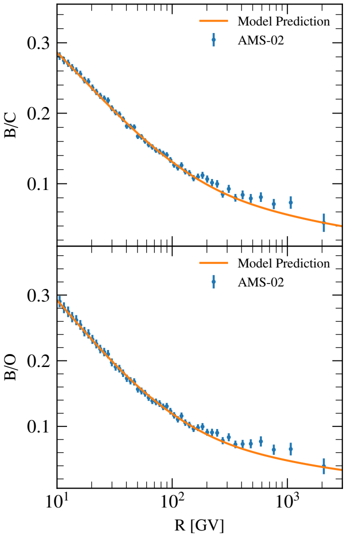

[Schroer et al. 2021, PRD]

Fit to light Ratios

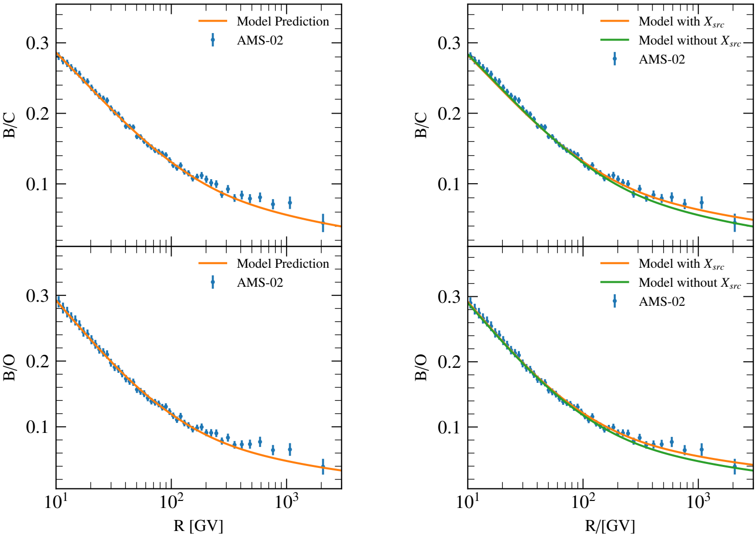

[Schroer et al. 2021, PRD]

He and H Results

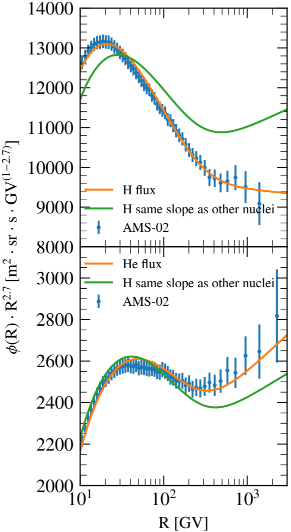

[Schroer et al. 2021, PRD]

- H and He require a different slope than other nuclei and each other, confirms result of previous study [Evoli et al. 2019] and independently confirmed by [Weinrich et al. 2020]
- Puzzling result as even theories that explain different slope of H and He predict same slope of He and heavier nuclei [Malkov et al. 2012]
- Raises the question: Is there an observable trend of the acceleration slope with particle mass?

Our Results

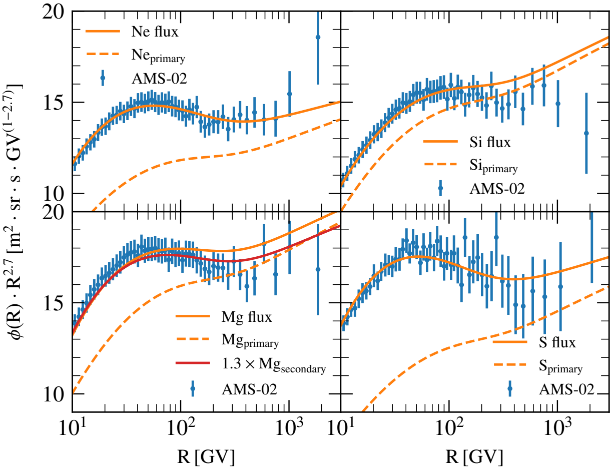

- Requiring the same slope leads to reasonably good fits
- Possible tensions can be lifted with cross-section uncertainties (see Mg)

[Schroer et al. 2021, PRD]

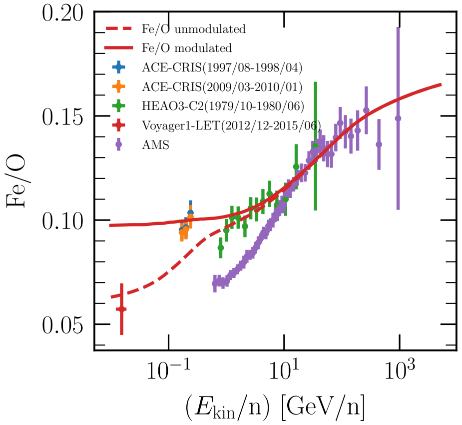

- Our model is compatible with all available data except AMS-02
- Additionally: AMS-02 data incompatible with HEAO3-C2 data in same energy range
- Fe data might require to incorporate a new or so far neglected effect into our model

[Schroer et al. 2021, PRD]

Possible Caveats

So far we tested different possible shortcomings of our model:

- Iron suffers severe energy losses, maybe ionization or spallation are not properly accounted for.

Possible Caveats

So far we tested different possible shortcomings of our model:

- ~~Iron suffers severe energy losses, maybe ionization or spallation are not properly accounted for.~~ Ionization has to be 5 times higher or spallation 40% larger to obtain a somewhat better fit
- The spallation inside the halo could become important

Possible Caveats

So far we tested different possible shortcomings of our model:

- ~~Iron suffers severe energy losses, maybe ionization or spallation are not properly accounted for.~~ Ionization has to be 5 times higher or spallation 40% larger to obtain a somewhat better fit
- ~~The spallation inside the halo could become important~~ Effect of halogrammage stays of %-order for reasonable halo densities
- Maybe iron experiences slightly different solar modulation for some unknown reason.

Possible Caveats

So far we tested different possible shortcomings of our model:

- ~~Iron suffers severe energy losses, maybe ionization or spallation are not properly accounted for.~~ Ionization has to be 5 times higher or spallation 40% larger to obtain a somewhat better fit
- ~~The spallation inside the halo could become important~~ Effect of halogrammage stays of %-order for reasonable halo densities
- ~~Maybe iron experiences slightly different solar modulation for some unknown reason.~~ Iron would need a 70% stronger modulation potential without any theoretical motivation
- Iron could have another injection slope

Possible Caveats

So far we tested different possible shortcomings of our model:

- ~~Iron suffers severe energy losses, maybe ionization or spallation are not properly accounted for.~~ Ionization has to be 5 times higher or spallation 40% larger to obtain a somewhat better fit
- ~~The spallation inside the halo could become important~~ Effect of halogrammage stays of %-order for reasonable halo densities
- ~~Maybe iron experiences slightly different solar modulation for some unknown reason.~~ Iron would need a 70% stronger modulation potential without any theoretical motivation
- ~~Iron could have another injection slope~~ Does not give a satisfying fit either

Summary

- Bottom line: CR fluxes can be well explained by imposing a single injection slope for nuclei heavier than He compatible with the expectation of zeroth order diffusive shock acceleration
- Only exception: the Fe measurement, where additionally AMS-02 and HEAO3-C2 disagree with each other
- Limiting factor: cross sections, see Mg flux

Summary

- Bottom line: CR fluxes can be well explained by imposing a single injection slope for nuclei heavier than He compatible with the expectation of zeroth order diffusive shock acceleration
- Only exception: the Fe measurement, where additionally AMS-02 and HEAO3-C2 disagree with each other
- Limiting factor: cross sections, see Mg flux
- Everything is nicely explained assuming the grammage is accumulated during transport, but how solid is this picture?

Non-linear theory of CRs escaping a SNR

CR Acceleration at SNR

- In standard model: Most Galactic CRs ($E < 1\,\mathrm{PeV}$)are thought to originate from SNRs, so-called SNR paradigm
- In order to accelerate CRs to $\sim$PeV energies at SNR shocks, strong magnetic turbulence and field amplification is required
- Main candidate to provide this field amplification: CRs generating the non-resonant streaming instability [Bell 2004]
- Requirement in all models in the literature: CRs of the highest energy escape during the Sedov-Taylor phase in order to excite this instability and trap lower energy particles [Bell et al. 2013; Caprioli et al. 2009; Reville et al. 2009]
- Escape Flux from the shock can be obtained as:

$$\phi(E > E_2) = \frac{\eta \rho u^3}{\ln(E_{max}/E_0)} E^{-1}$$

corresponding to the injection term in the previous model

Source in the ISM

- Once particles leave the source they diffuse on Galactic scales
- interstellar magnetic field is coherent on scales of 10-50pc [Ptuskin et al. 2008]
- mean free path $\lambda = \frac{3D}{v} \approx 1 \cdot E_{\mathrm{GeV}}^{1/2}\,\mathrm{pc} \Rightarrow$ ballistic escape initially

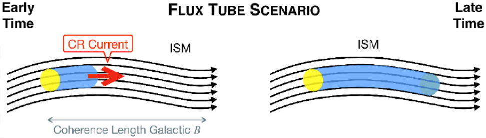

- $\Rightarrow$ CR escape preferentially along magnetic field lines and are ballistic above a certain energy $\Rightarrow$ 1D problem

Source in the ISM

- Once particles leave the source they diffuse on Galactic scales
- interstellar magnetic field is coherent on scales of 10-50pc [Ptuskin et al. 2008]
- mean free path $\lambda = \frac{3D}{v} \approx 1 \cdot E_{\mathrm{GeV}}^{1/2}\,\mathrm{pc} \Rightarrow$ ballistic escape initially

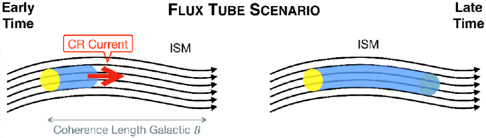

- $\Rightarrow$ CR escape preferentially along magnetic field lines and are ballistic above a certain energy $\Rightarrow$ 1D problem
- Under the flux tube approximation analytical solutions [Ptuskin et al. 2008; Malkov et al. 2013] were derived for a CR cloud expanding in a tube and exciting the resonant streaming instability, corresponding to a faded accelerator

Flux Tube Approximation

- Analytical and numerical solutions investigated the excitation of the **resonant streaming instability** [Malkov et al. 2013; D'Angelo et al. 2016; Nava et al.2016 & 2019; Recchia et al. 2022]
- Strong self-confinement in the circum-source region is found, becoming less effective towards higher energies
- As a result particles acquire a grammage in the circum-source region, while being trapped
- Estimates of this grammage range from it being negligible [Nava et al. 2019; Recchia et al. 2022] to being significant [D'Angelo et al. 2016]
- Strongly depends on relevant damping mechanisms

Non-resonant Streaming Instability

- Inject a flux of particles into a flux tube with the injected flux = flux escaping the shock
- Growth Condition: [Bell 2004]

$$\boxed{\frac{\phi_{CR}(E > E_0)}{c} E_0 \gg \frac{B_0^2}{4\pi}}$$

Non-resonant Streaming Instability

- Inject a flux of particles into a flux tube with the injected flux = flux escaping the shock
- Growth Condition: [Bell 2004]

$$\boxed{\frac{\phi_{CR}(E > E_0)}{c} E_0 \gg \frac{B_0^2}{4\pi}}$$

- For typical, young SNR $\boxed{\frac{4\pi \phi_{CR} E_0}{c B_0^2} \approx 100}$ [Schroer et al. 2021, ApJL]
- very fast growing mode $\gamma_{max}^{-1} \approx 1.1(\mathrm{E}/2.5\mathrm{TeV})\,\mathrm{yr}$, saturates after $\sim 5 - 10\gamma_{max}^{-1}$
- happens in very short time compared to typical age of SNR $\sim 10^{4..6}\,\mathrm{yr}$

GSSI

Consequences

- When particles start to diffusive, number density and pressure increase
- $\Rightarrow$ pressure in CR exceeds gas pressure $\rightarrow$ breaks 1D geometry because overpressurized region will expand in transverse direction

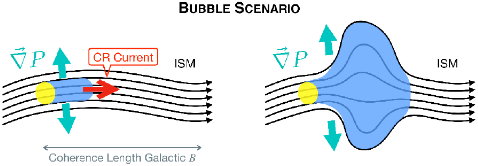

Simulation

- Hybrid particle in cell simulation with `dHybridR` [Haggerty & Caprioli 2019]
- Solve Maxwell equations and equations of motion for macroparticles
- Electromagnetic fields from the motion of the particles

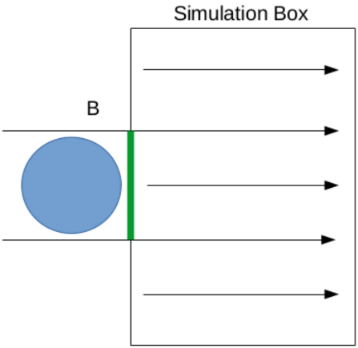

Movie

Evolution in 2D

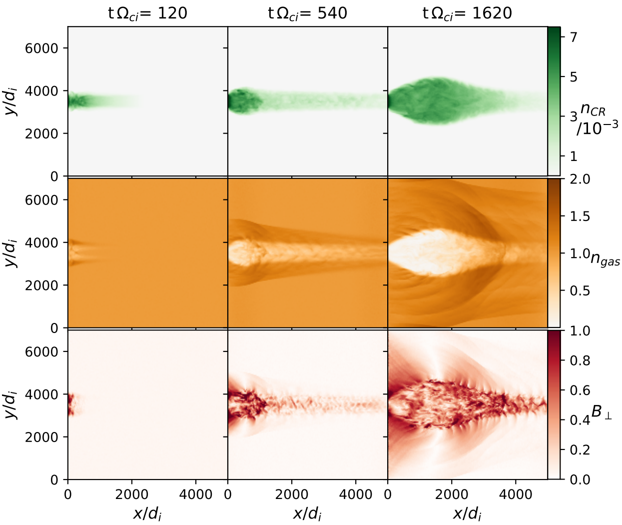

[Schroer et al. 2021, ApJL]

Evolution in 3D

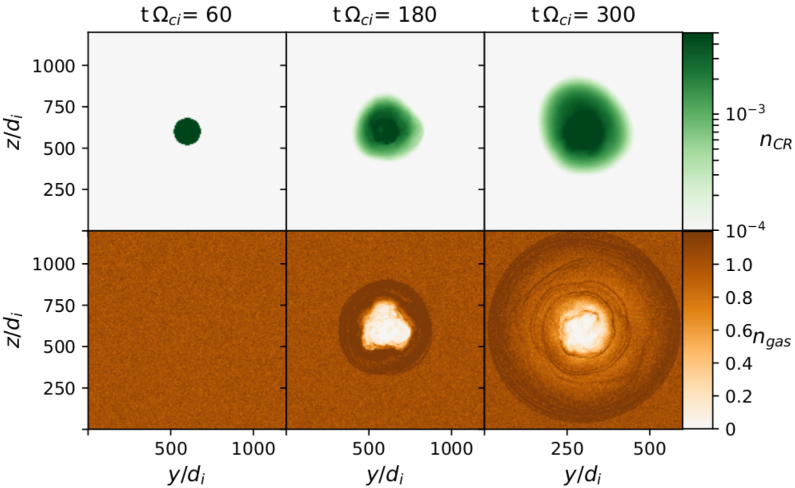

[Schroer et al. PoS(ICRC2021)]

Implications

- What are the observational consequences?

[Schroer et al. 2022, MNRAS]

Implications

- What are the observational consequences?
- Possible $\gamma-$ray morphology

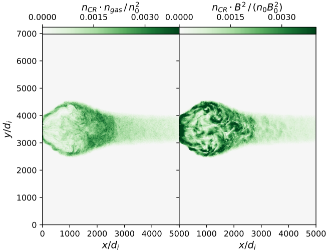

[Schroer et al. 2022, MNRAS]

Implications

- What are the observational consequences?
- Possible $\gamma-$ray morphology

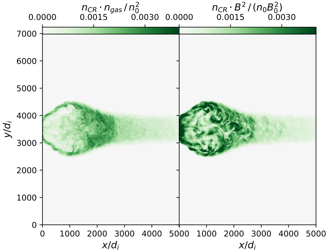

- Strong particle trapping influences the grammage accumulated by the particles
- Strongly dependent on achieved suppression of diffusion coefficient ξ and the gas density inside the bubble w.r.t. the ISM density η

$$\frac{X_{bubble}}{X_{Galactic}} \approx \frac{3 \times 10^{-1} \eta}{(\xi / 10^{-2})} \left(\frac{L}{50pc} \right)^2$$

- $\Rightarrow$ With $\eta = 1$ this gives $\sim 10\%$, contributes an additional grammage component to the fits of CR nuclei, but not the major part

[Schroer et al. 2022, MNRAS]

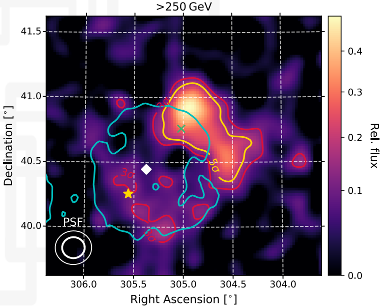

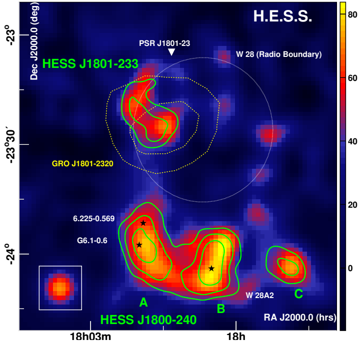

- Hints for strongly reduced diffusion coefficient observed near SNRs [Fujita et al. 2009; Gabici et al. 2010]
- Difficult task to detect due to specific necessary conditions, like presence of nearby molecular clouds

[MAGIC Collaboration 2010; HESS Collaboration 2008]

Summary

- We have seen that large energy densities and strong gradients close to sources modify the source environment
  $\Rightarrow$ We found a reduced diffusion coefficient and a cavity in the background gas
- Candidates for similar effects might be other sources, e.g., PWNe

TeV Halos

Observations and Motivation

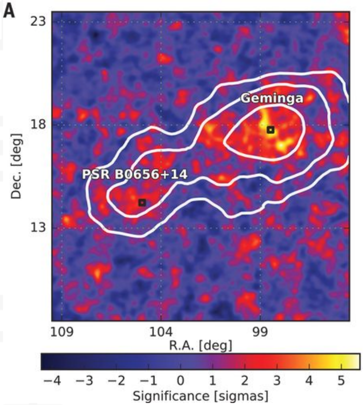

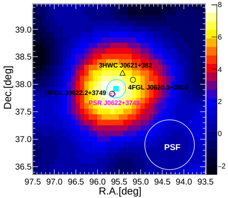

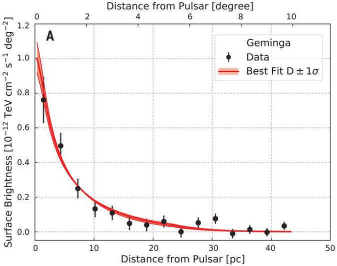

- Hints for strongly reduced diffusion coefficients observed in extended region around at least three PWNe

[HAWC Collaboration 2017; LHAASO Collaboration 2021]

Open Questions

- Many open Questions:
  - What is the origin of the suppressed diffusion? [Evoli et al. 2018; Mukhopadhyay & Linden 2021; Fang et al. 2019]
  - How large is the suppressed diffusion region? [Di Mauro et al. 2019]
  - How strong is the suppression?
  - How common are these objects? [Giacinti et al. 2020; Sudoh et al. 2019, Martin et al. 2022]

Open Questions

- Many open Questions:
  - What is the origin of the suppressed diffusion? [Evoli et al. 2018; Mukhopadhyay & Linden 2021; Fang et al. 2019]
  - How large is the suppressed diffusion region? [Di Mauro et al. 2019]
  - How strong is the suppression?
  - How common are these objects? [Giacinti et al. 2020; Sudoh et al. 2019, Martin et al. 2022]
- Viability of theories of their origin depends on size and amount of suppression, existing theories have problems explaining the commonly adopted size $\sim 50\,\mathrm{pc}$ and suppression ~ 1000
- Results of population studies of PWNe explaining the e^+ fraction might be influenced by the presence of halos
  - Without halos rather steep $e^\pm$ spectra with mean spectral indices $\gamma \sim 2.8$ are inferred [Evoli et al. 2021] while multiwavelength studies suggest ~ 2.5 [Bucciantini et al. 2011; Torres et al. 2014]
    $\Rightarrow$ effect of a common halo?

Model

- Goal: Investigate effect of halo around Geminga on the spectral index of the released particle spectrum and critically reasses the halos properties
- Use Green function approach to solve transport equation of pairs analytically:

$$\frac{\partial n(E,r,t)}{\partial t} = \frac{1}{r^2}\partial_r(r^2 D(E,r)\partial_r n(E,r,t)) + \partial_E \left(b(E)n(E,r,t)\right) + Q(E,r,t)$$

- With two different diffusion coefficients, inside and outside of halo
- Boundary conditions: $n_{in}(r_0) = n_{out}(r_0)$ and $D_{in}\partial_r n_{in}|_{r=r_\mathbf{0}} = D_{out}\partial_r n_{out}|_{r=r_\mathbf{0}}$

Model

- Goal: Investigate effect of halo around Geminga on the spectral index of the released particle spectrum and critically reasses the halos properties
- Use Green function approach to solve transport equation of pairs analytically:

$$\frac{\partial n(E,r,t)}{\partial t} = \frac{1}{r^2}\partial_r(r^2 D(E,r)\partial_r n(E,r,t)) + \partial_E\left(b(E)n(E,r,t)\right) + Q(E,r,t)$$

- With two different diffusion coefficients, inside and outside of halo
- Boundary conditions: $n_{in}(r_0) = n_{out}(r_0)$ and $D_{in}\partial_r n_{in}|_{r=r_0} = D_{out}\partial_r n_{out}|_{r=r_0}$
- In the literature so far an incorrect two-zone model was used
  $\Rightarrow$ Difference becomes important for small halo size / large loss lengths or positron flux calculations [Osipov et al. 2020]

Injection

- Spectra of $e^{\pm}$ released by bow shock PWNe are well fit by broken power laws [Bykov et al. 2017; Bucciantini et al. 2010]

$$Q(E,t) = Q_0(t) e^{-\frac{E}{E_c(t)}} \begin{cases} \left(\frac{E}{E_b}\right)^{-\gamma_L}, & E < E_b \\ \left(\frac{E}{E_b}\right)^{-\gamma_H}, & E_b < E \end{cases}$$

- Typically: $\gamma_L \sim 1 - 1.9$ and $\gamma_H \sim 2.5$, $E_b \sim 300 - 1000\,\mathrm{GeV}$ and potential drop $E_c \approx 300\,\mathrm{TeV}$ for Geminga today
- Normalization related to spin-down luminosity

$$\epsilon L(t) = \epsilon L_0 \frac{(1 + t_{age}/\tau_0)^{\frac{n+1}{n-1}}}{(1 + t/\tau_0)^{\frac{n+1}{n-1}}} := \int \mathrm{d}E\, Q(E,t)$$

- Here we fix $E_b = 1\,\mathrm{TeV}$ for Geminga and $\gamma_L = 1.5$ because they are degenerate with the injection efficiency and vary only γ_H
- Conversion efficiency of viable solutions is required to be $< 100\,\%$

Halo Size

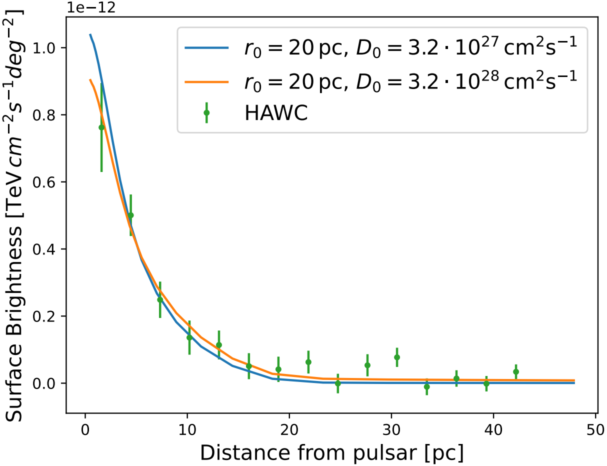

- Spatial profile can be reproduced by an escape-dominated scenario
- $D_{ISM} \approx 4 \cdot 10^{30}\,\mathrm{cm}^2/\mathrm{s}$

Different Magnetic Fields

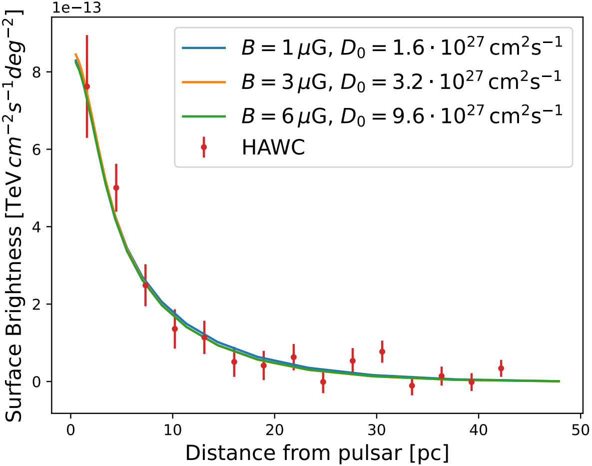

- Loss-dominated scenario: Spatial profile depends only on loss length for large enough halos ⇒ degenerate B and D_0

Total Flux

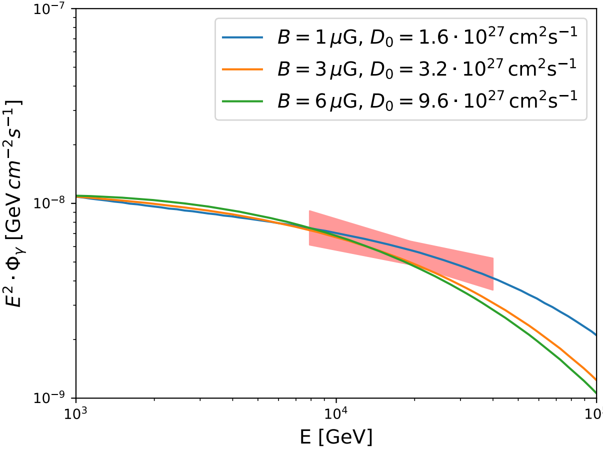

- Total flux gives way to disentangle equivalent spatial morphologies
- Low magnetic field seems preferred supporting results of X-ray study [Liu et al. 2019]

Protons

- Some models speculate that iron nuclei are stripped off the pulsar surface and are photodisintegrated into protons
  $\Rightarrow$ monoenergetic injection of protons at the pulsar [Venkatesan et al. 1997; Blasi et al. 2000; Amato & Arons 2006]:

$$Q_p(E_p, t) = \eta_p \dot{N}_{GJ}(t)\delta(E_p - E_c(t))\,,$$

- This leads to typically very hard spectra $\propto E^{-(n-1)/2}$ which gives E^{-1} for $n = 3$
- For the first time we consider that these protons can produce TeV γ-rays that might influence the inferred spectral index of electrons from observations
- Expected γ-rays dependent on gas density, here assumed as $1\,\mathrm{cm}^{-3}$

Protons

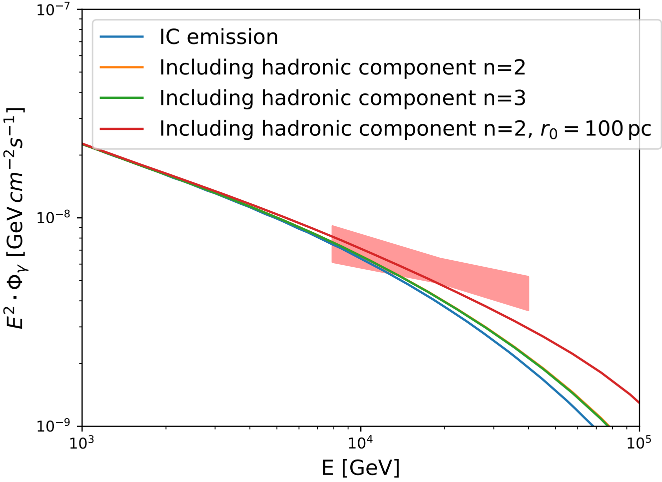

- Proton component might be important for large halos or small diffusion coefficients

Escape Flux

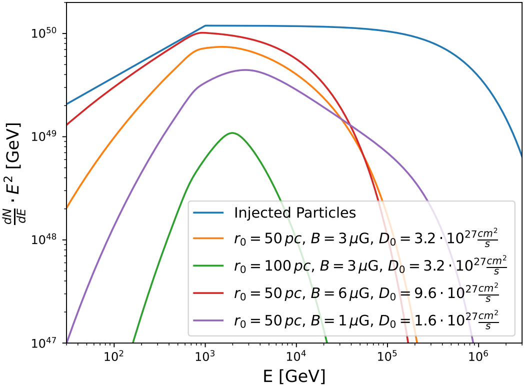

- Escape flux defined as: $\int_0^{t_{age}} \mathrm{d}t D \partial_r f|_{z=r_0}$
- With a low magnetic field the spectrum is steepened w.r.t. the injected one
- We obtain an effective cutoff after propagation that can be relevant for the positron fraction

Positron Flux

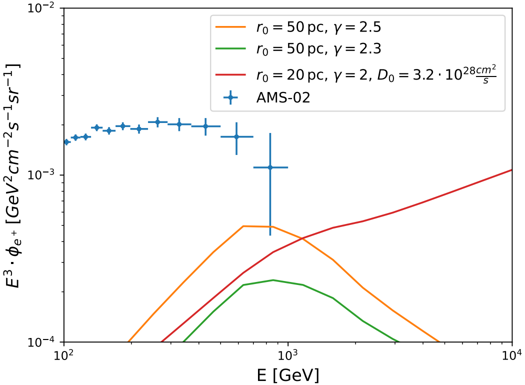

- Steeper spectra $\rightarrow$ higher contribution to local flux
- Data at higher energies will allow constrain on minimum halo size around Geminga
- New corrected model important

Conclusions and Outlook

Conclusions

- CR composition:

- able to reproduce flux of all elements with same injection spectrum except H and He which require a different slope
- Able to reproduce new data without refitting
- There seems to be an issue with Fe, that we still have to understand
- Currently no need for model modifications such as an additional source grammage or an extended disc model, but they could prove useful for future measurements

Future plans:

- **Study the impact of low diffusivity zones on the standard model $\Rightarrow$ model CR fluxes with an extended disc model**
- **Include antiprotons in our transport model**

Conclusions

- New insights about the escape of CRs from their sources:

- Current of escaping particles generates a non-resonant instability which slows down their escape
- Leads to the formation of CR bubbles around sources with reduced diffusivity
- Important implications:
  - Enhanced γ-ray emission from circumsource region
  - Accumulated grammage of trapped CRs might be significant for secondary-to-primary ratios but does not represent the major grammage component
    $\Rightarrow$ Supporting the standard model

Future plans:

- **Extend our work on SNR escape using MHD+PIC codes to achieve larger length and time scales**

Conclusions

- new insights about the Geminga TeV halo:

- Geminga halo has to be at least 20 pc large
- Diffusion coefficient is uncertain by a factor of ~ 10 but still requires suppression of ~ 100
- Taking into account the total flux, small magnetic field with intermediately steep spectra $\gamma_e \sim 2 - 2.3$ are able to explain observations
- Contribution of protons most likely negligible, except for very large halos and/or small diffusion coefficients (small B)
- Presence of halo steepens released spectra, a possible explanation for the inferred steep slope of the population study in [Evoli et al. 2021]

Future plans:

- **Investigate the origin of TeV halos: low diffusivity + small magnetic field seem similar to SNR bubble**

Publications

- *"Tracing the origin of low diffusivity and CR bubbles around sources"*, Schroer et al. 2021, PoS(ICRC2021)
- *"Dynamical Effects of Cosmic Rays on the Medium Surrounding Their Sources"*, Schroer et al. 2021, ApJL, 914, L13
- *"Intermediate-mass and heavy Galactic cosmic-ray nuclei: The case of new AMS-02 measurements"*, Schroer et al. 2021, PRD, 103, 123010
- *"Cosmic-ray generated bubbles around their sources"*, Schroer et al. 2022, MNRAS, 512, 1
- In preparation, Schroer et al. 2023

Appendix

CR nuclei

Our Model

One can rewrite as equation in terms of grammage and flux $I_a(E) = 4\pi A p^2 f_a(p)$:

$$\frac{I_a(E)}{X_a(E)} + \frac{\mathrm{d}}{\mathrm{d}E}\left(\left[\left(\frac{\mathrm{d}E}{dx}\right)_{ad} + \left(\frac{\mathrm{d}E}{dx}\right)_{ion,a}\right] I_a(E)\right)$$
$$+\frac{I_a(E)}{X_{\mathrm{cr,a}}} = 2h\frac{A_a p^2 q_a(p)}{\mu v} + \sum_{a'>a}\frac{I_{a'}(E)}{m}\sigma_{a'\to a}$$

- where we introduced the critical grammage $X_{\mathrm{cr,a}} := \frac{m}{\sigma_a}$ and the grammage traversed by nuclei a $X_a(E) := \frac{\mu v}{2v_A}\left(1 - e^{-\frac{v_A H}{D}}\right)$
- Without energy losses $I_a(E) \propto E^{-\gamma+2}$ for $X_a(E) \gg X_{\mathrm{cr,a}}$ and $I_a(E) \propto E^{-\gamma+2-\delta}$ for $X_a(E) \ll X_{\mathrm{cr,a}}$
- $\Rightarrow$ Secondary over primary ratios flat at low E and $\propto E^{-\delta}$ at high E
- Solutions only sensitive to ratio $\frac{H}{D}$

Fitting Parameters

- Spatial transport, including diffusion and advection, comprises 7 free-parameters: D_0, δ, v_A, H, R_b, $\Delta\delta$, s:

$$D(R) = 2v_A H + \beta D_0 \frac{(R/\mathrm{GV})^{\delta}}{[1 + (R/R_b)^{\Delta\delta/s}]^s} ,$$

  motivated by [Recchia et al. 2016]
- The injection efficiencies ϵ_a of the species H, He, C, N, O, Ne, Mg, Si, S and Fe
- Injection slope γ, assumed to be the same for all of them without any break
- Solar modulation potential ϕ
- Total of 19 parameters
- Restrict ourselves to $R > 10\,\mathrm{GV}$ to reduce the impact of low-energy effects

Cross sections

- Some isotopes are short-lived on Myr time scales and never leave the Galactic disc
  $\Rightarrow$ these isotopes are not propagated but taken into account as instantaneous decay
  $\Rightarrow$ ghost nuclei
- Example ^{22}Na with life time $\tau_d = 4.8\,\text{kyr}$:

$$\sigma^C_{X\rightarrow^{22}Ne} = \sigma_{X\rightarrow^{22}Ne} + \sigma_{X\rightarrow^{22}Na}\,\mathcal{B}(^{22}Na \rightarrow^{22} Ne) \qquad (2)$$

- In general, $\tau_d \ll \tau_{res}$ is an energy dependent statement $\Rightarrow$ Assumption might break at high energies for certain nuclei

Thick Disc Model

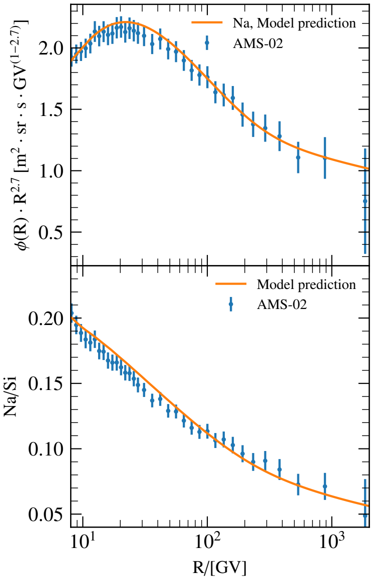

Thick Disc Model

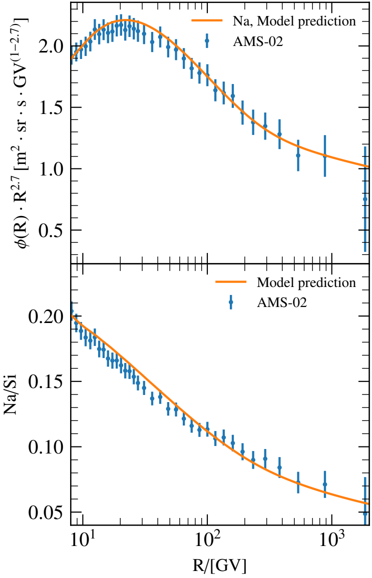

- Some short-lived nuclei like ^{22}Na are treated as ghost nuclei (instantaneously decaying inside the disc), but might leave the disc at high rigidities
- I developed an extended-disc model to properly capture this effect

Thick Disc Model

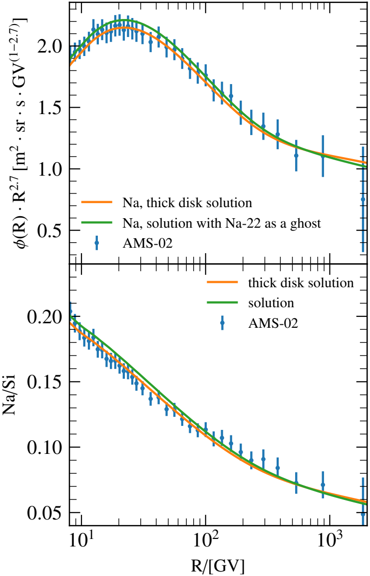

- Some short-lived nuclei like ^{22}Na are treated as ghost nuclei (instantaneously decaying inside the disc), but might leave the disc at high rigidities
- I developed an extended-disc model to properly capture this effect
- Current data only marginally sensitive to this effect

Predictions

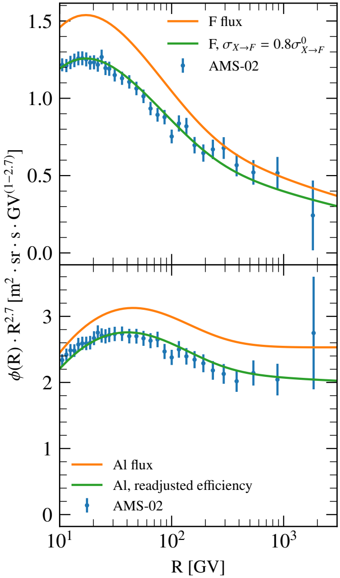

CALET Fe Measurement

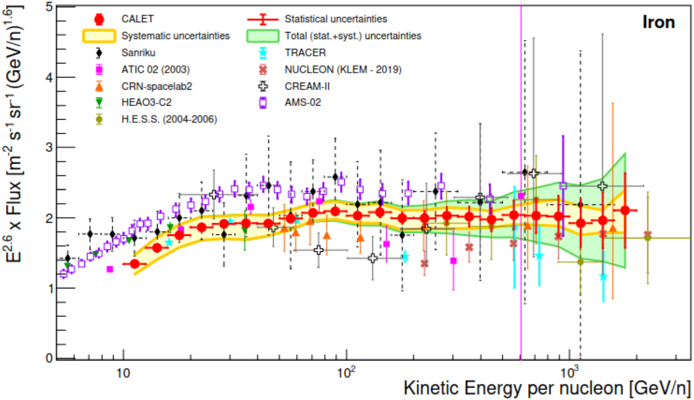

- CALET measurement shows different normalization than AMS-02, but confirms slope
- However does not cover the part of the spectrum where we see the large deviations from our model and other experiments

[CALET Collaboration 2021]

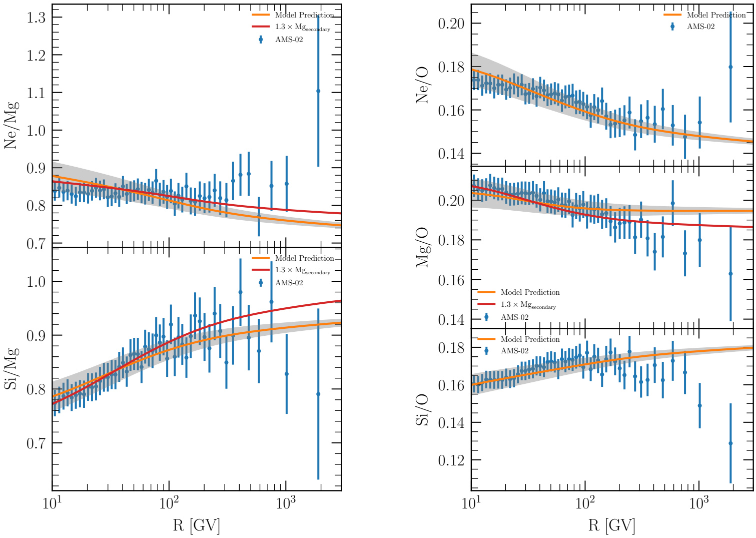

[Schroer et al. 2021, PRD]

SNR Escape

Power Spectrum

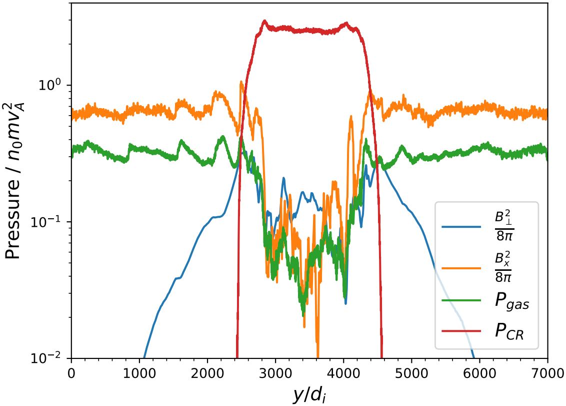

[Schroer et al. 2021, MNRAS]

Power Spectrum

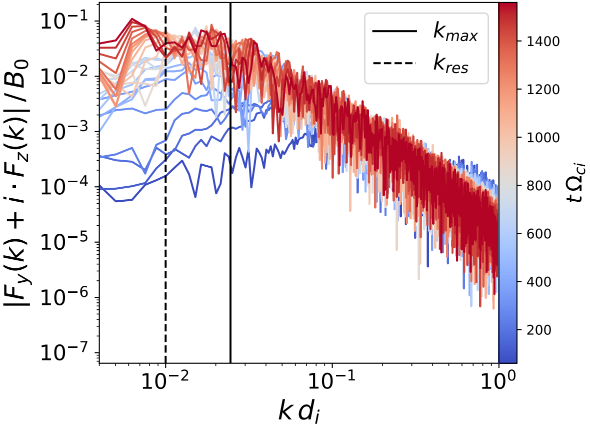

[Schroer et al. 2021, MNRAS]

Power Spectrum

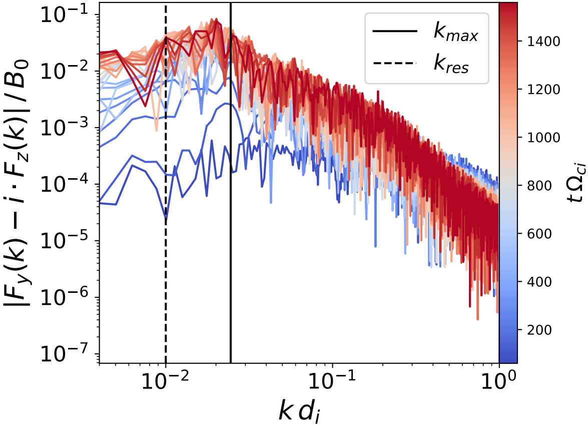

[Schroer et al. 2021, MNRAS]

Power Spectrum

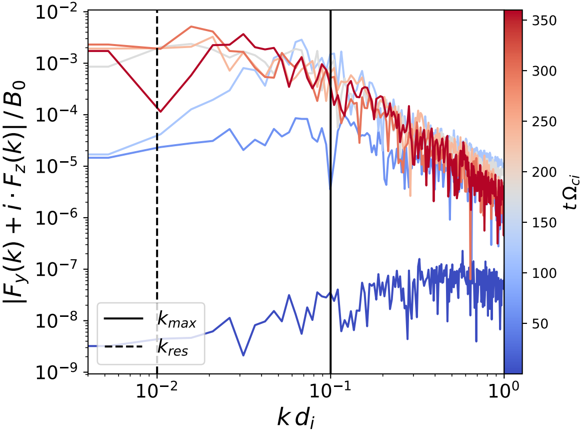

[Schroer et al. 2021, MNRAS]

Power Spectrum

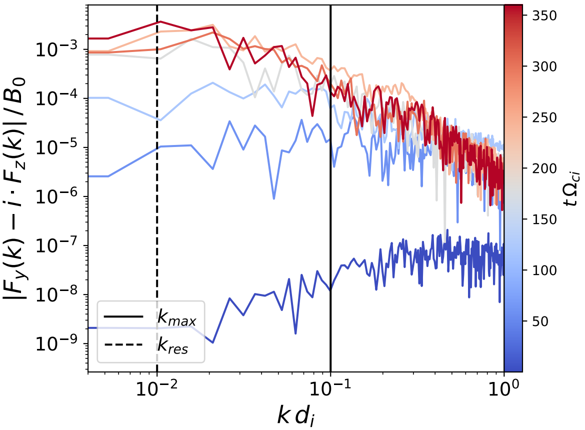

[Schroer et al. 2021, MNRAS]

dHybridR

$$\frac{\partial f_s}{\partial t} + \mathrm{v} \cdot \nabla f_s + \frac{q_s}{m_s}(\mathrm{E} + \frac{\mathrm{v}}{c} \times \mathrm{B}) \cdot \nabla_v f_s = 0$$

$$\frac{\partial \mathrm{B}}{\partial t} = -c\nabla \times \mathrm{E}$$

$$\frac{\partial \mathrm{E}}{\partial t} = c\nabla \times \mathrm{B} - 4\pi \mathrm{J}$$

$$\nabla \cdot \mathrm{B} = 0$$

$$\nabla \cdot \mathrm{E} = \sum_s q_s n_s$$

The electron number density is fixed to the ion number density $n_e = n_i$ to ensure quasi neutrality of the system resulting in $\nabla \cdot \mathrm{E} = 0$ and $\mathrm{J} = en_i(\mathrm{V}_i - \mathrm{V}_e)$

dHybridR

Macro particles are propagated according to:

$$m_i \frac{\mathrm{d}\gamma \mathrm{v}}{\mathrm{d}t} = q\mathrm{E} + \frac{q}{c}\mathrm{v} \times \mathrm{B}$$

The electric field is obtained via

$$\mathrm{E} = -\frac{\mathrm{V}_e}{c} \times \mathrm{B} - \frac{1}{en}\nabla P_e = -\frac{\mathrm{V}_i}{c} \times \mathrm{B} + \frac{\mathrm{J}}{enc} \times \mathrm{B} - \frac{1}{en}\nabla P_e$$

assuming: $v_A \ll c$, $n_{CR} \ll n_i$ and $V_{bkg} \ll c$.

Simulation Details

- $c/v_A = 20$
- $5000 \times 7000\, d_i^2$, with 7500×10500 cells ($1200 \times 1200 \times 1200\, d_i^3$, with 1440×1440×1440 cells in 3D)
- gas: $N_{ppc} = 4$, CRs: $N_{ppc} = 16$, $n_{CR} = 0.0133$ (0.01 in 3D), $p_{CR} = 100\, mv_A$, $r_{g,i} = d_i$, i.e. $\beta_i = 2v_{th,i}^2/v_A^2 = 2$
- Reproduce the ratio of energy densities of CR particles and thermal energy $\sim (n_{\rm CR}/n_0)(c/v_A)^2\gamma \sim 26$
- Bell condition fulfilled by: $\sigma = \frac{n_{CR}}{n_i}\frac{p_{min} v_d}{m_i v_A^2} \approx 5$, in 3D $\sigma \approx 20$
- Growth rate $\gamma_{max} = \frac{n_{CR}}{2n_i}\frac{v_d}{v_A} \approx \frac{1}{40}$ ($\frac{1}{10}$ for 3D)

SNR estimate

- $L_{CR} = \frac{\epsilon E_{SN}}{T_S}$
- Used quantities: $E_{SN} = 10^{51}\,\text{erg},\ T_S = 300\,\text{years},\ R_S = 3\,\text{pc},\ \epsilon = 0.1,\ B_0 = 3\,\mu\text{G},\ E_{max} = 1\,\text{PeV},\ E_{min} = 1\,\text{GeV}$

$$\phi_{CR}(E > E_0) = \frac{L_{CR}}{2\pi R_s^2 \Lambda E_0}$$

- For typical, young SNR $\boxed{\frac{4\pi\phi_{CR}E_0}{cB_0^2} \approx 100}$

SNR Estimate

- The differential particle flux in energy that escapes is $Q_{esc}(E,t) = Q_s(E,t)E\delta(E - E_{max}(t))$ with $Q_s(E,t)$ the flux injected and accelerated at the shock
- $\eta L(t) = \frac{1}{2}\eta\rho u^3 = \int_{E_0}^{E_{max}} \mathrm{d}E E Q_s(E,t)$
- $\phi(E > E_2) = \int_{E_2} \mathrm{d}E' Q_{esc}(E') = Q_0(t_E)E^{1-\alpha}\Theta(E - E_2)$

$$\phi_{CR}(E' > E) = \frac{\eta\rho u^3}{\Lambda}E^{-1} = \frac{\eta E_{SN} u}{\pi R^3 \Lambda}E^{-1} = \frac{2\eta E_{SN}}{5\pi R^2 T_{ST}\Lambda}E^{-1}$$

with $\rho u^2 \pi R^3 = E_{SN}$ and $R/u = \frac{5}{2}T_{SN}$

TeV halo

Solution

$$n(E, r, t) = \int_0^{t-t_{BS}} \mathrm{d}t_0 \frac{b(E(t_0))}{b(E)} Q(E(t_0), t - t_0 + t_{BS}) H(r, E, t_0)$$

Two Zone Model

- $$H(r,E,t) = \int_0^\infty \mathrm{d}\psi \frac{\xi e^{-\psi}}{\pi^2 \lambda_0^2 (A^2(\psi) + B^2(\psi))} \begin{cases} \frac{\sin(2\sqrt{\psi}\frac{r}{\lambda_0})}{r} & , 0 < r < r_0 \\ A(\psi)\frac{\sin(2\sqrt{\psi}\frac{r\xi}{\lambda_0})}{r} + B(\psi)\frac{\cos(2\sqrt{\psi}\frac{r\xi}{\lambda_0})}{r} & , r \geq r_0, \end{cases}$$

  with

  $$\begin{aligned} A(\psi) = \xi \cos(2\sqrt{\psi}\frac{r_0}{\lambda_0}) \cos(2\xi\sqrt{\psi}\frac{r_0}{\lambda_0}) \\ + \sin(2\sqrt{\psi}\frac{r_0}{\lambda_0}) \sin(2\xi\sqrt{\psi}\frac{r_0}{\lambda_0}) \\ + \frac{\lambda_0}{2\sqrt{\psi} r_0}(\frac{1-\xi^2}{\xi} \sin(2\sqrt{\psi}\frac{r_0}{\lambda_0}) \cos(2\xi\sqrt{\psi}\frac{r_0}{\lambda_0}) \end{aligned}$$

  and

  $$B(\psi) = \frac{\sin(2\sqrt{\psi}\frac{r_0}{\lambda_0}) - A(\psi)\sin(2\xi\sqrt{\psi}\frac{r_0}{\lambda_0})}{\cos(2\xi\sqrt{\psi}\frac{r_0}{\lambda_0})}$$

GeV halo

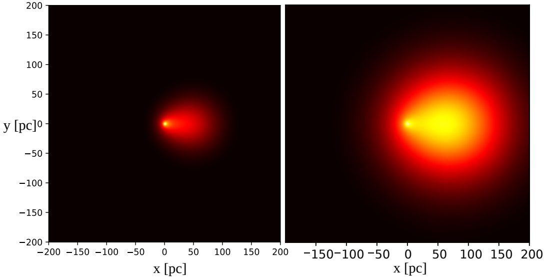

200
150
100
50
0
−50
−100
−150
−200
y [pc]
−200 −150 −100 −50 0 50 100 150 200
x [pc]
−150 −100 −50 0 50 100 150 200
x [pc]

Different Injection Slope

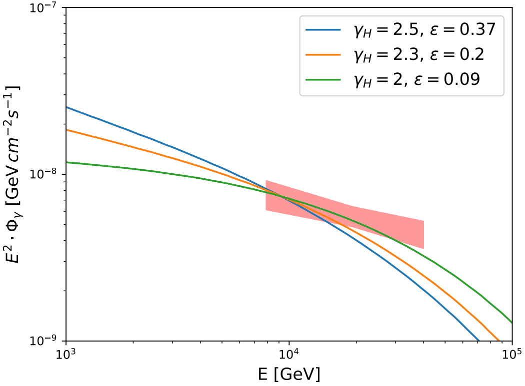

Different Injection Slope

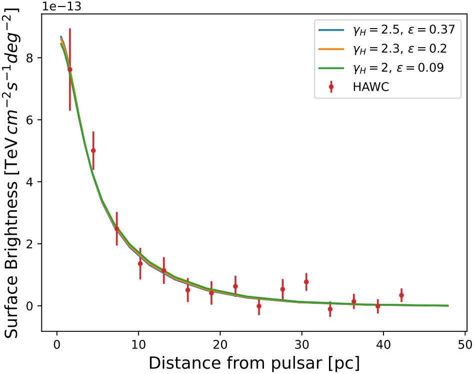

Different ISRF

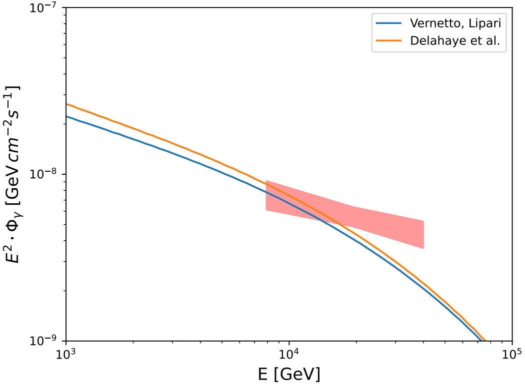

Wrong Two Zone Model

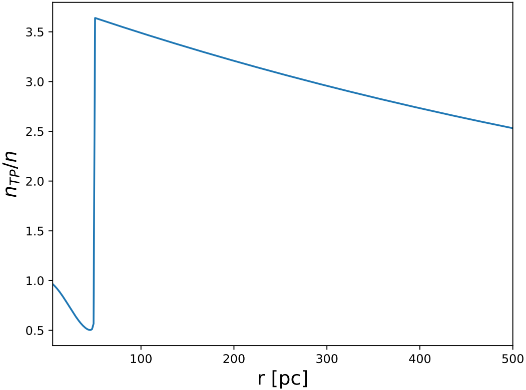

Positron Flux

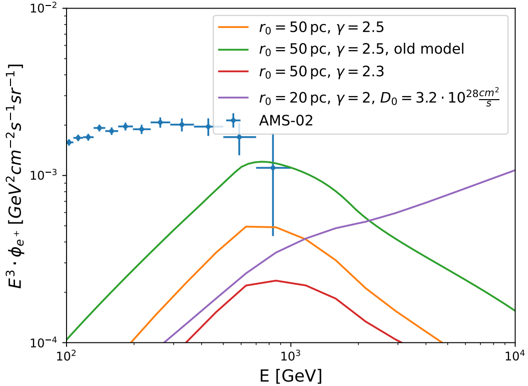

Emission

$$\phi_\gamma(E_\gamma) = \frac{1}{4\pi d^2} \int_0^{E_{max}} \mathrm{d}E_e \frac{dN_e}{dE_e}(E_e) \frac{dN_\gamma}{hd\nu dt}(E_e)$$

- Total Flux:

$$\Phi_\gamma(E) = 2\pi \int_{-d}^{\infty} \mathrm{d}l \int_0^{r_{max}} \mathrm{d}r r \phi_\gamma(E_\gamma, r, l)$$